HHS Public Access

Author manuscript

Mol Cancer Ther. Author manuscript; available in PMC 2017 June 01.

Published in final edited form as:

Mol Cancer Ther. 2016 June ; 15(6): 1353–1363. doi:10.1158/1535-7163.MCT-15-0332.

Edelfosine Promotes Apoptosis in Androgen Deprived Prostate Tumors by Increasing ATF3 and Inhibiting Androgen Receptor Activity

Thirupandiyur S. Udayakumar[1], **Radka Stoyanova**[1], **Mohammed M. Shareef**[1], **Zhaomei Mu**[2], **Sakhi Philip**[1], **Kerry L. Burnstein**[3], and **Alan Pollack**[1]

[1]Department of Radiation Oncology, Sylvester Cancer Center, Miller School of Medicine, University of Miami, Miami, FL

[2]Department of Medical Oncology, Thomas Jefferson University, Philadelphia, PA

[3]Department of Molecular and Cellular Pharmacology, University of Miami, Miami, FL

Abstract

Edelfosine is a synthetic alkyl-lysophospholipid (ALP) that possesses significant antitumor activity in several human tumor models. Here, we investigated the effects of edelfosine combined with androgen deprivation (AD) in LNCaP and VCaP human prostate cancer cells. This treatment regimen greatly decreased cell proliferation compared to single agent or AD alone resulting in higher levels of apoptosis in LNCaP compared to VCaP cells. Edelfosine caused a dose-dependent decrease in AKT activity, but did not affect the expression of total AKT in either cell line. Furthermore, edelfosine treatment inhibited the expression of androgen receptor (AR) and was associated with an increase in activating transcription factor 3 (ATF3) expression levels, a stress response gene and a negative regulator of AR transactivation. ATF3 binds to AR after edelfosine + AD and represses the transcriptional activation of AR as demonstrated by prostate specific antigen (PSA) promoter studies. Knockdown of ATF3 using siRNA-ATF3 reversed the inhibition of PSA promoter activity, suggesting that the growth inhibition effect of edelfosine was ATF3 dependent. Moreover, expression of AR variant 7 (ARv7) and TMPRSS2-ERG fusion gene were greatly inhibited after combined treatment with AD and edelfosine in VCaP cells. *In vivo* experiments using an orthotopic LNCaP model confirmed the anti-tumor effects of edelfosine + AD over the individual treatments. A significant decrease in tumor volume and PSA levels were observed when edelfosine and AD were combined, compared to edelfosine alone. Edelfosine shows promise in combination with AD for the treatment of prostate cancer patients.

Correspondence: Alan Pollack, MD, PhD, Chair and Sylvester Professor, Department of Radiation Oncology, University of Miami Miller School of Medicine, 1475 NW 12th Ave Suite 1500 (D-31), Phone: 305-243-4916; Cell: 305-775-1780, APollack@med.miami.edu.

Note: Supplementary data for this article are available at Molecular Cancer Therapeutics Online (http://mct.aacrjournals.org/).

Disclosure of Potential Conflicts of Interest

Kerry L. Burnstein reports receiving a commercial research grant from Amgen. No other potential conflicts of interest were disclosed by other authors.

Keywords

edelfosine; androgen deprivation; ATF3; prostate cancer

Introduction

Androgen deprivation (AD) is the most common treatment for locally advanced and metastatic prostate cancer, with more recent findings supporting the significance of new drugs affecting androgen metabolism and androgen receptor (AR) signaling in prolonging survival. AD improves overall survival when combined with radiation for intermediate and high risk localized disease (1). The major reason for prostate cancer mortality is progression while receiving AD and development of castrate-resistant prostate cancer (CRPC) (2, 3). Our previous studies have shown that the addition of targeted therapy to AD may enhance and prolong AD response, and extend survival in pre-clinical models (4, 5). Here, we studied the efficacy of combining AD with the ether lipid, edelfosine.

Edelfosine (ET-18-O-CH3) is a prototypal synthetic alkyl-lysophospholipid (ALP) with potent anti-tumor effects. Although the mechanism of action of edelfosine is not fully elucidated, two main targets have been reported: (i) plasma membrane, where edelfosine interacts with lipid rafts, and (ii) endoplasmic reticulum (ER), where edelfosine can induce ER stress and inhibit phosphatidylcholine biosynthesis (6). Edelfosine induces apoptosis selectively in tumor cells by disrupting numerous signal transduction pathways (i.e., AKT) that are associated with cell survival (7). Preclinical studies of edelfosine did not show significant systemic side effects or bone marrow toxicity (8). Other in vitro and in vivo studies revealed that edelfosine caused cytotoxic effects in leukemic cells and solid tumors, but not in normal cells suggesting selectivity for cancer (9, 10). Clinical trials with edelfosine showed very good tolerability and safety (11).

Several signaling pathways are deregulated in prostate cancer cells, including the phosphatidylinositol-3-kinase (PI3K)AKT pathway, which mediates the effects of a variety of extracellular signals and is crucial for the maintenance and proliferation of prostate cells (12). PI3K is the major activator of AKT resulting in AKT translocation to the plasma membrane where it is phosphorylated at two key residues, Thr308 and Ser473 (13). There is also a direct connection between PI3K-AKT activity and AR signaling during the development of AD resistance (14); although, precise mechanisms remain to be determined. Functional loss of PTEN is associated with increased AKT-1 phosphorylation, higher Gleason grade, advanced stage, and poor prognosis (15), predicting disease recurrence after primary treatment (16). Reports suggest that PI3K signaling may play a critical role, allowing prostatic cancer to maintain continued growth in low-androgen environments (17).

One mechanism associated with CRPC involves alternate splicing of AR truncated variants, termed ARvs (3). AR splice variant 7 (ARv7) is the most commonly expressed ARv in human tissues (18). Expression levels of ARv7 are correlated with biochemical relapse and decreased survival in advanced prostate cancer patients. In addition, AR target genes such as TMPRSS2 undergo frequent chromosomal rearrangements in prostate cancer with members of the E-twenty six (ETS) transcription factor family (ERG or ETV1), which is associated

with the transition from high-grade prostatic intraepithelial neoplasia lesions to invasive carcinoma (19).

Aberrant expression of the ATF3 gene is frequently associated with prostate cancer (20). ATF3 interacts and regulates AR transactivation via its transcription factor domain (basic leucine zipper - bZIP) (21, 22). ATF3 knockout mice display increased proliferative activity of the prostate epithelium and prostatic hyperplasia (21). Loss of ATF3 expression increased both the transcription of androgen-dependent genes and the ability of prostate cancer cells to grow in AD medium. ATF3 has also been shown to activate or repress the expression of genes by binding to their promoters (23). However, details of its function as a stress response mediator remain largely unknown. In this study, we investigated the potential of edelfosine to intensify effects from AD in promoting cell killing and tumor growth inhibition in androgen-sensitive human prostate cancer cells via modulation of several key factors such as AKT, AR, ARv7, ATF3 and TMPRSS2-ERG and their interaction.

Materials and Methods

Cell culture and reagents

LNCaP, VCaP and 22RV1 cells were grown in Dulbecco's modified Eagle's medium (DMEM/F12) in the presence of 10% fetal bovine serum (FBS), 1% L-glutamine, and 1% penicillin-streptomycin (CM - complete medium). Cells were authenticated by RADIL (University of Missouri-Columbia, Columbia, MO), using short tandem repeat markers. AD treatment was achieved by culturing the cells in DMEM/F12 medium containing 10% charcoal-stripped serum (AD medium) for 3 days (4). Antibodies against total AKT (# 9272), p-AKT (AKT S473, # 4058) were purchased from Cell Signaling Technologies (Beverly, MA); ATF3 (sc-22798), AR polyclonal antibody (N-20; sc-816) and β-actin (# 7210) from Santa Cruz Biotechnology (Dallas, TX); ARv7 (# AG10008) from Precision Antibody (Columbia, MD); ERG (CM 421A) from Biocare Medical (Concord, CA) and horseradish peroxidase (HRP)-conjugated secondary antibodies from Amersham Pharmacia Biotech (Piscataway, NJ); R1881 (# NLP00500) from Perkin Elmer (Waltham, MA); control siRNA (sc-37007) and ATF3 siRNA (sc-44283) from Santa Cruz Biotechnology (Dallas, TX) and ATF3 plasmid (# 26115) from Addgene (Cambridge, MA). Edelfosine was a generous gift from Dr. Vladimir Khazak (Fox Chase Cancer Center, Philadelphia, PA). Edelfosine stocks were prepared in 0.01 M phosphate buffered saline (PBS) and stored at −20° C until use.

Real time cell proliferation assay

Cell proliferation was examined using real-time monitoring in LNCaP and VCaP cells grown in CM or AD medium. Briefly, background measurements were taken after adding 50 μl of the either CM or AD medium to the wells of the E-Plate from xCELLigence System (ACEA Biosciences, Inc., San Diego, CA). Then 2×10^4 cells were seeded in 16 well E-plates. Cell proliferation was continuously monitored every hour for a period of 72 h after different doses of edelfosine treatment (0, 1, 2.5, 5, 10 and 20 μM). Control groups received PBS vehicle (0.01 M). Cell sensor impedance is expressed as the Cell Index, a measure of adhesion across the individual well. Start and end times were selected for each treatment

during the log growth phase and used to calculate doubling time with real-time cell analyzer (RTCA) Software v1.2 (ACEA Biosciences, San Diego, CA).

Apoptosis assays

Annexin V staining and caspase 3/7 activity assays were used to analyze apoptotic cell death as described previously (4). For annexin V assay, LNCaP cells were cultured in complete or AD medium in 6 well tissue culture plates for 3 days, then treated with different concentrations of edelfosine (0, 5 and 10 μM) and incubated at 37 °C for 24 h. Cells were harvested and stained using the Guava Nexin kit (Guava Technologies Inc, Burlingame, CA). Cell populations were analyzed by flow cytometry on a GuavaPC personal flow cytometer and the data were processed using CytoSoft software. For caspase activity assay, LNCaP and VCaP cells were cultured in complete or AD medium for 3 days, then treated with different concentrations of edelfosine (0, 5 and 10 μM) for 24 h. For ATF3 knockdown study, cells were pre-transfected for 18 h with 10 nM of siATF3 (siRNA for ATF3) or control siRNA in the presence of lipofectin reagent in 6 well tissue culture plates. Cells transfected with siATF3 were then exposed to edelfosine (0, 5, 10 μM for LNCaP, LNCaP + AD and 0, 5 μM for VCaP, VCaP + AD). Cells (floating and attached) were harvested following 24 h of treatment. Caspase 3/7 activity was determined using the Apo-ONE™ homogeneous caspase 3/7 assay kit (Promega, Madison, WI). Harvested cells (2×10^4) in 50 μl culture medium were mixed with 50 μl homogeneous caspase-3/7 reagent in a 96 well plate and incubated at room temperature for 24 h. The activity was measured according to the manufacturer's instructions using a fluorescent plate reader (Beckman Coulter, Danvers, MA).

Western blot analysis

The whole-cell lysates from AD and edelfosine treated LNCaP and VCaP cells were prepared as described previously (24). In brief, cells were cultured in complete or AD medium for 3 days in 10 cm tissue culture dishes, then treated with different concentration of edelfosine (0, 2.5, 5 and 10 μM). PBS (0.01 M) vehicle was added to the control group. For ATF3 knockdown studies, cells were pre-transfected for 18 h with 10 nM ATF3 siRNA or control siRNA in the presence of lipofectin reagent. Cells were either harvested at different time points or 24 h post-treatment, lysed in lysis buffer (50 mM Tris-HCL, pH 6.8, 2% sodium dodecyl sulfate [SDS] with protease inhibitor), and sonicated for 30 seconds on ice. Total proteins (30 μg/lane) from whole-cell lysates were subjected to SDS-PAGE electrophoresis and probed with specific antibodies. The dilutions used for p-AKT was 1:500. For total AKT, AR, ARv7, ERG, ATF3 and β-actin 1:1000 dilution was used. The immunoblots with antibodies were rocked on a shaker overnight at 4°C. The membranes were washed and incubated with an anti-rabbit or mouse horseradish-peroxidase conjugated secondary antibody (1:5000 dilution) for 1 h at room temperature. Immunoreactive proteins were visualized by the chemiluminescence reagents.

Quantitative real-time PCR (qRT-PCR)

For qRT-PCR, total RNA (500 ng) was transcribed into cDNA using qScript™ cDNA Synthesis Kit (Quanta Biosciences, Gaithersburg, MD). Real-time RT-PCR reactions were performed using qScript™ One-Step SYBR® Green qRT-PCR kit (Quanta Biosciences,

Gaithersburg, MD) and the following TMPRSS2-ERG fusion gene-specific primers: TMPRSS2-ERG RT forward, 5'-CAGGAGGCGGAGGCGGA-3'; TMPRSS2-ERG RT reverse, 5'-GGCGTTGTAGCTGGGGGTGAG-3' and human GAPDH forward, 5'-GAGTCAACGGATTTGGTCGT-3', and reverse, 5'-TTGATTTTGGAGGGATCTCG-3' were used (25). qRT-PCR reactions were run on an ABI Prism 7000 Sequence Detection System (Thermoscientific, Grand Island, NY). Data were analyzed using the ΔΔCt method (26), where target gene expression is normalized to the housekeeping gene by taking the difference between Ct values for target gene and housekeeping gene (ΔCt). This value was then compared to that of the normalized control sample (ΔΔCt). The fold change was then determined by the formula: $2^{-\Delta\Delta Ct}$.

Reporter gene assays and transfections

All transfections using the lipofectin transfection reagent (Life Technologies, Grand Island, NY) were done according to the manufacturer's instructions. LNCaP cells were cultured in AD medium for 3 days. For luciferase assay, cells were plated at a density of 2×10^5 cells in 6 well plates for 24 h. Before transfection, medium was replaced with serum free DMEM/F12 medium. Cells were transfected with 3 μg/well of prostate specific antigen (PSA) or androgen response element (ARE) luciferase reporter (27), siATF3 (10 nM) and renilla luciferase (30 ng/well) or CMV-ATF3 (3 μg/well). After 3 h incubation with DNA/lipofectin complexes, cells were refed with 2% AD medium. The cells were treated with 10 nM of R1881 (dissolved in ethanol) and 5 μM edelfosine. Control wells received equal amount of vehicle (ethanol and 0.01 M PBS). Cells were harvested 24 h after transfection, lysed, and assessed for luciferase activity using the dual luciferase assay kit (Promega Corp., Madison, WI). Luciferase values were normalized using renilla luciferase expression. The data represent mean ± SD (Standard Deviation) from three independent experiments.

Reverse Transcriptase-Polymerase Chain Reaction (RT-PCR)

For RT-PCR, LNCaP cells with various treatment groups were transfected with PSA reporter construct (3 μg), siATF3 (10 nM) and CMV-ATF3 (3 μg). After 3 h incubation with DNA/lipid complexes, cells were refed with 2% AD medium. The cells were treated with 10 nM of R1881, and 5 μM edelfosine. Twenty four hour after transfection RNA was isolated by using RNeasy mini kit (Qiagen, Valencia, CA) and quantified by Nano-Drop 2000c spectrophotometer (Thermoscientific, Wilmington, DE). For the RT-PCR analysis, first-strand cDNA was synthesized from total RNA (2 μg) using oligo-(dT)-20 and a ThermoScript RT-PCR System (Thermoscientific, Grand Island, NY). PSA primers (forward 5'-CCCTCCCCTTCCACAGCTCTGGGT-3' and reverse 5'-CCGCCCCTGCCCTGCTGGCACCC-3') were synthesized by IDT (Integrated DNA Technologies, Inc., Coralville, Iowa). PCR amplification reaction was carried out using Phusion™ High Fidelity DNA polymerase kit. A portion (10 μl from a 20 μl reaction) of the PCR reaction product was electrophoresed on a 1.5% agarose gel containing ethidium bromide. Electrophoresed and ethidium bromide stained PCR products from RT–PCR reactions were recorded under UV-transillumination by the Gel Doc XR system (Bio-Rad, Hercules, CA) normalized with respect to the amount of GAPDH product.

In vivo treatment groups, tumor volume and PSA measurements

Male athymic nude mice, 4-8 weeks old were obtained from Harlan (Indianapolis, IN). Aseptic techniques were used for injections and implantation of prostate tumor cells in the prostates of nude mice as described previously (4, 5, 28). In brief, LNCaP cells (5×10^5) were implanted into the dorsal prostate. Two weeks after orthotopic implantation, serum PSA levels were measured weekly by an enzymatic immunoassay kit according to the manufacturer's protocol on an IMX analyzer (Abbott Labs, Abbott Park, IL). When the PSA level was approximately 3.0 – 8.0 ng/mL, mice were treated orally by gavage. At this point bilateral orchiectomy was performed under anesthesia on the animals in the AD groups (4) 3 days prior to edelfosine treatment. A total of eight groups of animals (n = 9 - 13) were studied: PBS (control) and three concentrations of edelfosine was given at doses 5, 10 and 20 mg/kg body weight, 3 days per week for 10 weeks, with and without AD. Tumor volumes (TV), determined by magnetic resonance imaging (MRI), and serum PSA levels were obtained weekly after treatments. The efficacy of the treatment was assessed by MRI volume and PSA levels at 6 weeks. For MRI, imaging was performed at a field strength of 7 T in a vertical wide-bore (10 cm) magnet using a Bruker DRX spectrometer (Bruker Biospin, Karlsruhe, Germany) as previously reported (4, 5, 28).

Immunoprecipitation

To study the interaction between AR and ATF3, we immunoprecipitated protein extract with polyclonal AR or ATF3 antibody followed by ATF3 or AR immunoblot analysis. Briefly, edelfosine (5 μM) treated LNCaP cell lysates (200 μg) were incubated each with 1 μg (AR/N-20 or ATF3/H-90, Santa Cruz, Dallas, TX) of AR or ATF3 antibody overnight followed by incubation with protein G-Sepharose beads (Life Technologies, Grand Island, NY) at 4°C for 1 h. Immunocomplexes were washed three times with lysis buffer and were denatured by treatment with SDS sample-loading buffer at 100 °C for 10 minutes followed by immunoblotting with ATF3 or AR specific antibodies. Proteins were visualized using an enhanced chemiluminescence system (GE Healthcare Bio-science, Piscataway, NJ).

Immunohistochemical analysis

Orthotopic LNCaP tumor bearing mice were treated with edelfosine (20 mg/kg/3 times per week). Tumors were excised 24 h following treatment, fixed in formalin, embedded in paraffin, and processed for immunohistochemistry. Expressions levels of p-AKT, ATF3 and caspase 3/7 were analyzed by immunohistochemistry, as described previously (28). The slides were scanned with a VS120-SL microscope (Olympus, Pittsburgh, PA) and the images were captured using VS-ASW-FL 2.6, virtual software imaging system.

Data analysis and statistics

For *in vitro* studies, statistical analyses were carried out by one way ANOVA, Bonferroni test. For *in vivo* studies the time series for each animal was fitted with a single exponential model, as described previously (5). Student's *t* test was applied to the estimates of TV and PSA levels at 6 weeks and to their doubling times. Percentage of mice with TV < 100 mm^3 and/or PSA < 25 ng/ml from the experimental pairs, PBS and edelfosine, with and without

AD were placed in 2 × 2 contingency tables and tested for significance using the chi-square test. For all statistical tests, a p value of ≤ 0.05 was considered significant.

Results

Edelfosine inhibits LNCaP cell proliferation

Real-time cell electronic sensing (RT-CES), a noninvasive and real-time monitoring of live prostate cancer cell status (29), was used to assess prostate cancer cell growth, death and morphology changes. LNCaP cells were seeded and cultured in CM or AD conditions (Fig. 1A and B) for 24 h followed by treatment with edelfosine (0, 1, 2.5, 5, 10 and 20 μM). The cells were monitored every hour for 72 h. We did not see any difference in the cell index (CI) in the treatment groups before the treatment started. As expected, LNCaP cells exhibited reduced growth under AD conditions compared to CM. For cells grown in CM and treated with edelfosine, a dose dependent decrease in cell numbers was observed. Under AD conditions, even the lowest dose of edelfosine greatly decreased cell numbers (Fig. 1B). Edelfosine was most effective when combined with AD conditions. Similar results were observed with VCaP cells. (Supplementary Fig. S1).

Edelfosine causes apoptosis in LNCaP and VCaP that is accentuated by AD

Annexin V and caspase-3/7 activation are regarded as early apoptotic markers (30). Annexin V positive (apoptotic) LNCaP cells significantly increased following 10 μM edelfosine treatment in both CM and AD media (Fig. 2A). Apoptotic effects of edelfosine were most striking in AD conditions in which there was a dose dependent increase in apoptosis by edelfosine at 5 and 10 μM (Fig. 2A). Onset of cell death is predicated by the level of caspase 3/7 activity in cancer cells. The degree of basal caspase 3/7 activation was higher in LNCaP cells (Fig. 2B) than in VCaP cells (Fig. 2C) in both CM and AD medium. Edelfosine treatment resulted in increased caspase 3/7 activity in both cell lines in CM and AD media. As observed for Annexin V staining, edelfosine increased caspase 3/7 most effectively under AD conditions.

ATF3 has a key role in the cell death response of LNCaP and VCaP to edelfosine plus AD

Cellular stress, including DNA damage and oxidative stress, can rapidly induce ATF3 (31). ATF3 has been shown to directly bind AR and repress AR-mediated gene expression (21). We had an interest in ATF3 for these reasons and that edelfosine induces a stress response and increase apoptosis (32). The expression level of ATF3 increased with AD and was further increased when AD was combined with edelfosine. A dose dependent increase in ATF3 expression was observed in both cell lines when edelfosine was increased from 2.5 to 5 μM under both CM and AD conditions (Fig. 2D). When edelfosine was administered at 10 μM in combination with AD, ATF3 remained significantly elevated over no edelfosine (AD alone), but was at lower levels than at 5 μM, possibly related to the increased cell death seen under these conditions.

To confirm the role of ATF3 in the cell death response to AD and edelfosine, knockdown was achieved with co-transfection of siATF3. Caspase 3/7 activity was significantly ($p < 0.05$) reduced in both cell lines (Fig. 2B and C) when siATF3 was combined with AD and

edelfosine. The knockdown of ATF3 after siATF3 was confirmed by Western blot analysis (Fig. 2E). Cells transfected with control siRNA did not show any inhibitory effect (Fig. 2E, F and Supplementary Fig. S2). These findings indicate that the higher levels of cell death achieved in LNCaP and VCaP prostate cancer cells when edelfosine was combined with AD was mediated at least in part to up-regulation of ATF3.

Edelfosine and AD decrease AR and ARv7 protein levels

We have shown previously that levels of AR, p53 and p21 proteins are decreased when cells are grown in AD medium for 3 days (4). The AKT pathway modulates AR function (33) and protects prostate cancer cells from apoptosis induced by AD (34). Here we tested the effect of AD + edelfosine on AKT activation because edelfosine has been shown to act on the AKT pathway (35). Figure 3 shows that edelfosine down regulated p-AKT and AR in LNCaP and VCaP cells. Edelfosine inhibited the phosphorylation of p-AKT in both cell lines in a dose (Fig. 3A) dependent manner without affecting total AKT expression. As displayed in Supplementary Fig. S3, increasing inhibition of p-AKT after 10 μM edelfosine in LNCaP cells was observed over an 18 h period, with or without AD. Moreover, p-AKT levels were significantly decreased when AD was combined with edelfosine, relative to that seen in the absence of AD. The reduction in cell proliferation from edelfosine + AD and the parallel decrease in p-AKT expression suggest that AKT activity might have a role in apoptotic response to AD.

We next examined the effects of edelfosine and AD on the constitutively active AR isoform, ARv7, which is present in VCaP cells because this prevalent AR variant may contribute to the restoration of AR transcriptional activity in CRPC (18, 36). Prior studies have shown that depletion of ARv7 or total AR by siRNA, reduces the expression of PSA, cell proliferation and TMPRSS2 (18). The TMPRSS2-ERG fusion gene is a well-known target of AR (37). Therefore, we explored the expression of ARv7 and TMPRSS2-ERG after edelfosine ± AD in VCaP cells grown *in vitro*. A dose dependent inhibition of ARv7 and ERG was evident after edelfosine, treatment, with or without AD. This inhibition was higher when AD was combined with 10 μM of edelfosine. Moreover, the knockdown of ATF3 using siATF3 reversed the inhibition of both ARv7 and its TMPRSS2-ERG fusion gene target (Fig. 3B). Similar results were observed with ERG expression at the mRNA level by real-time PCR (Fig. 3C). Notably, ARv7 expression was also inhibited in CRPC cell line 22RV1 after edelfosine treatment (Supplementary Fig. S3B), and the inhibition was more pronounced when edelfosine was combined with AD. As expected, we did not detect ERG expression in 22RV1 cells. These data show significantly favorable alterations in AR, ARv7 and TMPRSS2-ERG fusion gene expression when AD is combined with edelfosine that is mediated in large part to ATF3.

ATF3-AR interaction is increased by edelfosine plus AD

ATF3 interacts with AR and represses AR activity (21). Here, we sought to confirm that this interaction occurs to a greater degree after edelfosine + AD. AR-specific antibodies were used in an immunoprecipitation assay (IP) to pull down the AR protein complexes from whole-cell extracts after edelfosine treatment at 2.5 and 5 μM in LNCaP cells. For the IP, anti-AR antibodies but not IgG control antibodies from edelfosine treated LNCaP cells

resulted in an ATF3 band migrating at ~21 kDa (Fig. 3D) confirming the interaction between AR and ATF3 that was dose dependent on edelfosine. The AR/ATF3 interaction was increased 2 fold (by densitometry analysis) by edelfosine at 5 μM, as compared to the untreated cells. The interaction was confirmed when ATF3 antibodies were used for IP (Fig. 3E).

Edelfosine mediates AR transcriptional activity in part through ATF3

The PSA gene is another direct target of AR (38). To determine whether the edelfosine-mediated increase in ATF3 represses AR transcriptional activity, we co-transfected PSA luciferase reporter constructs (39) in LNCaP cells grown in AD medium with or without androgen (R1881), followed by edelfosine treatment (Fig. 4A). Under these conditions, PSA luciferase activity was dramatically reduced 24 h after edelfosine treatment. PSA promoter activity was considerably restored when ATF3 was depleted via siATF3 (Fig. 4A) indicating a role for ATF3 in inhibiting AR-mediated transcription. We also observed that when ATF3 was overexpressed using a CMV-ATF3 construct in the presence of androgen supplementation (R1881), PSA transactivation was significantly lower. Further, LNCaP cells were transfected with PSA-luciferase reporter, control siRNA, siATF3 or CMV-ATF3 as described above and the PSA expression was measured by ELISA in the culture supernatant after 24 h. A significant decrease in PSA protein expression was observed with edelfosine + AD ± androgen supplementation (Supplementary Fig. S4) compared to AD alone. Semi-quantitative RT-PCR (Fig. 4B) confirmed the expression levels of PSA mRNA in a parallel study with the same treatment groups as in PSA luciferase reporter experiments (Fig. 4A). Also, knockdown of endogenous ATF3 using siRNA showed no significant difference in PSA levels compared to control siRNA and R1881-treated controls. Similar results were observed using an ARE-luciferase construct (27) in reporter assays (Supplementary Fig. S5). Taken together, these results show that edelfosine efficiently increases ATF3 and the ATF3/AR interaction, which is associated with decreased levels of AR and its transcriptional activity.

Edelfosine treatment suppresses the growth of orthotopic LNCaP tumors

LNCaP tumors grown orthotopically in nude mice (5, 28) were used to examine the *in vivo* effects edelfosine + AD. Orthotopically grown tumors mimic the stromal environment which is an advantage to assessing prostate tumor response to therapy. Tumor growth inhibition was determined by MRI-based TV and serum PSA measurements for 20 weeks. Edelfosine treatment was started 3 days post orchiectomy by gavage at 5 mg/kg, 10 mg/kg or 20 mg/kg given 3-days/week for 10 weeks. Edelfosine alone and edelfosine + AD resulted in tumor growth inhibition in a dose-dependent manner (Fig. 5A and B; Table 1). The graphs represent changes in average TV (± SEM; standard error of the mean) over the course of 20 weeks. Similar trends were observed for PSA values (Table 1). The greatest effect was seen with edelfosine 20 mg/kg + AD.

The effect of edelfosine (20 mg) and AD on absolute PSA levels and TVs are shown in Table 1, along with the fraction of mice with LNCaP tumors with PSA levels of < 25 ng/ml and TVs of < 100 mm^3 at 6 weeks, and a combination endpoint, defined as the percentage of mice meeting both requirements for PSA and TV thresholds. The combination resulted in

smaller TVs and lower PSAs relative to all other groups, including edelfosine or AD alone. Our prior results have shown that there was a significant association between MRI-based TV and serum PSA in orthotopic prostate cancer models (5).

We investigated the levels of p-AKT, ATF3 and caspase activity in tumor tissues from mice treated with AD + edelfosine by immunohistochemistry (Fig. 5C). Expression of activated p-AKT was notably decreased in orthotopic prostate tumor sections when AD + edelfosine were combined. Likewise, caspase 3/7 and ATF3 expression were the highest under these conditions.

Discussion

For high risk and metastatic prostatic adenocarcinoma, AD is a mainstay of treatment due to the sensitivity of tumors to androgen for proliferation and tumor cell survival (3). However, with time, castration-resistant disease emerges in the vast majority and is a precursor of mortality (40). New therapeutic agents that enhance AD response, delay the emergence of castrate resistance and/or delay progression after castrate resistance are needed. In the present study, we carried out experiments to determine if edelfosine sensitizes prostatic carcinoma cells to AD. Edelfosine belongs to the family of synthetic ALPs that includes miltefosine, perifosine and erucyl phosphocholine (10). These drugs act on cell membranes by inhibiting phosphatidylcholine biosynthesis (32), and have been shown to sensitize tumor cells to chemotherapy and/or radiotherapy (41).

The AKT/protein kinase B signaling pathway is implicated in ALP-mediated apoptosis (7). In our studies, edelfosine decreased cell proliferation in androgen-deprived medium and increased cell death, as measured by Annexin V and caspase-3/7 activation. Prior studies have shown that lymphoma cells undergo apoptosis in response to edelfosine (42). Others have shown in breast cancer that edelfosine induced apoptosis by inhibiting ERK1/2, p38 MAPK, and AKT activation (7). Other reports suggest that edelfosine targets membrane lipid rafts via the recruitment of proapoptotic Fas/CD95 death receptor into the rafts and AKT inactivation (43). Here, we report a substantial reduction in p-AKT when edelfosine was combined with AD, indicating that this regimen inhibited AKT activity. Inhibition of AKT by edelfosine was probably due to the disruption of the structure and signaling within lipid rafts, preventing AKT recruitment to the membrane (10). Since the AKT pathway modulates AR function (33) and protects prostate cancer cells from apoptosis induced by AD, we investigated the contribution of this mechanism to the additive effects of edelfosine and AD.

Our data demonstrates that edelfosine reduced the expression of AR when combined with AD in a dose dependent manner. Many reports have shown that AR activity may be altered by aberrant expression of AR-binding proteins (44). Following activation by androgen binding, AR translocates to the nucleus and various regulators of AR such as chromatin remodeling complexes, transcription factors, and co-activator/co-repressors interact with AR to regulate its transcriptional activity (44). We hypothesized that edelfosine and AD induce a stress response and that factors induced by that response have a role suppressing AR activity. ATF3 has been shown by others to play a critical role in genotoxic stress-induced apoptosis

in embryonic fibroblast cells (45) supporting the pro-apoptotic role of ATF3. Since ATF3 binds to AR and represses AR transcriptional activity (21) the reduction of AR activity could be due to induced expression and binding to AR.

Activated transcription factor 3 (ATF3) is a stress response gene that is de-regulated in different types of cancers including prostate cancer (46). ATF3 is frequently induced under cellular stress (DNA damage) and plays a crucial role in cell homeostasis (23, 47). We observed an increase in ATF3 expression after edelfosine treatment; the increase was more robust when edelfosine was combined with AD. Using siATF3 to knockdown ATF3 we confirmed that edelfosine + AD mediated cell death in prostate cancer cells is indeed related to ATF3 modulation (Fig. 2). Moreover, elevated ATF3 in response to edelfosine + AD interacted with AR more substantively (Fig. 3D/E), which could then prevent AR from binding to AREs. Indeed, edelfosine decreased transcriptional activity of AR through ATF3 as evidenced using PSA and ARE reporter constructs, as well as assessing PSA and ERG mRNA regulation. This inhibition in the reporter activities was reversed by siATF3 knockdown, suggesting that the augmented inhibitory effects seen with the combination of edelfosine + AD over that of individual treatments was associated with ATF3 levels and activity.

In our orthotopic LNCaP *in vivo* studies, the combination of edelfosine + AD caused a synergistic reduction in LNCaP orthotopic TV (Fig. 5, Table 1). Edelfosine, when combined with AD, resulted in a more than 7 fold decrease in TV and PSA levels as compared to either of the treatment given alone. Immunohistochemical analysis under these conditions also confirmed increased expression of caspase 3/7, a decrease in activated p-AKT and an increase in ATF3, corroborating with the *in vitro* data.

AR splice variant ARv7 is associated with drug resistance in CRPC patients treated with the antiandrogens enzalutamide and the androgen synthesis inhibitor abiraterone (48, 49). We observed that full length-AR, ARv7 and the AR target TMPRSS2-ERG fusion gene were significantly inhibited after combined treatment with edelfosine + AD in VCaP cells. Reports suggest that restoration of AR transcription is mediated by elevated levels of ARv7, which may promote prostate tumor growth and drug resistance by the expression of specific set of AR target genes (18). The fusion TMPRSS2-ERG gene has been implicated in migration, invasion and metastasis (37). The expression of ARv7 or the fusion gene TMPRSS2-ERG product ERG increase tumor response to AD and tumor aggressiveness, and drugs like edelfosine that have potential to improve patient outcome by downregulating these genes when combined with AD therapy.

In summary, we report for the first time that edelfosine significantly augments the response of androgen-sensitive prostate cancer cells to AD *in vitro* and *in vivo*, resulting in reduced tumor cell proliferation and increased apoptosis. Mechanistically, edelfosine + AD modulates AR function by decreasing p-AKT and inducing ATF3 (Fig. 5D). In particular, ATF3 binds to AR and represses AR signaling that results in downstream effects on AR transcription targets. The potentiation of AD activity by edelfosine has significant implications in the management of patients with high risk or metastatic prostate cancer.

Supplementary Material

Refer to Web version on PubMed Central for supplementary material.

Acknowledgements

Edelfosine was a generous gift from Dr. Vladimir Khazak (Fox Chase Cancer Center, Philadelphia).

Grant Support: This publication was supported in part by Grants from the National Cancer Institute CA101984 (A. Pollack) and CA132200 (K. Burnstein), Department of Defense (US Army Medical Research Grant) PC020427 (A. Pollack) and Bankhead-Coley Cancer Research Program of Department of Health, State of Florida 09BW-10 (A. Pollack). The contents are solely the responsibility of the authors and do not necessarily represent the official views of the National Cancer Institute, US Department of Defense, and Florida Department of Health.

References

1. Matsumoto K, Hagiwara M, Tanaka N, Hayakawa N, Ishida M, Ninomiya A, et al. Survival following primary androgen deprivation therapy for localized intermediate- or high-risk prostate cancer: comparison with the life expectancy of the age-matched normal population. Medical oncology. 2014; 31:979. [PubMed: 24781338]
2. Koo KC, Park SU, Kim KH, Rha KH, Hong SJ, Yang SC, et al. Prognostic Impacts of Metastatic Site and Pain on Progression to Castrate Resistance and Mortality in Patients with Metastatic Prostate Cancer. Yonsei medical journal. 2015; 56:1206–12. [PubMed: 26256961]
3. Karantanos T, Corn PG, Thompson TC. Prostate cancer progression after androgen deprivation therapy: mechanisms of castrate resistance and novel therapeutic approaches. Oncogene. 2013; 32:5501–11. [PubMed: 23752182]
4. Mu Z, Hachem P, Hensley H, Stoyanova R, Kwon HW, Hanlon AL, et al. Antisense MDM2 enhances the response of androgen insensitive human prostate cancer cells to androgen deprivation in vitro and in vivo. Prostate. 2008; 68:599–609. [PubMed: 18196567]
5. Stoyanova R, Hachem P, Hensley H, Khor LY, Mu Z, Hammond ME, et al. Antisense-MDM2 sensitizes LNCaP prostate cancer cells to androgen deprivation, radiation, and the combination in vivo. Int J Radiat Oncol Biol Phys. 2007; 68:1151–60. [PubMed: 17637390]
6. Czyz O, Bitew T, Cuesta-Marban A, McMaster CR, Mollinedo F, Zaremberg V. Alteration of plasma membrane organization by an anticancer lysophosphatidylcholine analogue induces intracellular acidification and internalization of plasma membrane transporters in yeast. J Biol Chem. 2013; 288:8419–32. [PubMed: 23344949]
7. Na HK, Surh YJ. The antitumor ether lipid edelfosine (ET-18-O-CH3) induces apoptosis in H-ras transformed human breast epithelial cells: by blocking ERK1/2 and p38 mitogen-activated protein kinases as potential targets. Asia Pac J Clin Nutr. 2008; 17(Suppl 1):204–7. [PubMed: 18296338]
8. Gajate C, Mollinedo F. Biological activities, mechanisms of action and biomedical prospect of the antitumor ether phospholipid ET-18-OCH(3) (edelfosine), a proapoptotic agent in tumor cells. Curr Drug Metab. 2002; 3:491–525. [PubMed: 12369895]
9. Runge MH, Andreesen R, Pfleiderer A, Munder PG. Destruction of human solid tumors by alkyl lysophospholipids. J Natl Cancer Inst. 1980; 64:1301–6. [PubMed: 6929370]
10. Mollinedo F, de la Iglesia-Vicente J, Gajate C, Estella-Hermoso de Mendoza A, Villa-Pulgarin JA, de Frias M, et al. In vitro and In vivo selective antitumor activity of Edelfosine against mantle cell lymphoma and chronic lymphocytic leukemia involving lipid rafts. Clin Cancer Res. 2010; 16:2046–54. [PubMed: 20233887]
11. Chee KG, Longmate J, Quinn DI, Chatta G, Pinski J, Twardowski P, et al. The AKT inhibitor perifosine in biochemically recurrent prostate cancer: a phase II California/Pittsburgh cancer consortium trial. Clin Genitourin Cancer. 2007; 5:433–7. [PubMed: 18272025]
12. Bitting RL, Armstrong AJ. Targeting the PI3K/Akt/mTOR pathway in castration-resistant prostate cancer. Endocr Relat Cancer. 2013; 20:R83–99. [PubMed: 23456430]
13. Franke TF. PI3K/Akt: getting it right matters. Oncogene. 2008; 27:6473–88. [PubMed: 18955974]

14. Mikhailova M, Wang Y, Bedolla R, Lu XH, Kreisberg JI, Ghosh PM. AKT regulates androgen receptor-dependent growth and PSA expression in prostate cancer. Advances in experimental medicine and biology. 2008; 617:397–405. [PubMed: 18497063]
15. Ayala G, Thompson T, Yang G, Frolov A, Li R, Scardino P, et al. High levels of phosphorylated form of Akt-1 in prostate cancer and non-neoplastic prostate tissues are strong predictors of biochemical recurrence. Clin Cancer Res. 2004; 10:6572–8. [PubMed: 15475446]
16. Kreisberg JI, Malik SN, Prihoda TJ, Bedolla RG, Troyer DA, Kreisberg S, et al. Phosphorylation of Akt (Ser473) is an excellent predictor of poor clinical outcome in prostate cancer. Cancer Res. 2004; 64:5232–6. [PubMed: 15289328]
17. Mulholland DJ, Dedhar S, Wu H, Nelson CC. PTEN and GSK3beta: key regulators of progression to androgen-independent prostate cancer. Oncogene. 2006; 25:329–37. [PubMed: 16421604]
18. Liu LL, Xie N, Sun S, Plymate S, Mostaghel E, Dong X. Mechanisms of the androgen receptor splicing in prostate cancer cells. Oncogene. 2014; 33:3140–50. [PubMed: 23851510]
19. Perner S, Mosquera JM, Demichelis F, Hofer MD, Paris PL, Simko J, et al. TMPRSS2-ERG fusion prostate cancer: an early molecular event associated with invasion. Am J Surg Pathol. 2007; 31:882–8. [PubMed: 17527075]
20. Lapointe J, Li C, Higgins JP, van de Rijn M, Bair E, Montgomery K, et al. Gene expression profiling identifies clinically relevant subtypes of prostate cancer. Proc Natl Acad Sci U S A. 2004; 101:811–6. [PubMed: 14711987]
21. Wang H, Jiang M, Cui H, Chen M, Buttyan R, Hayward SW, et al. The stress response mediator ATF3 represses androgen signaling by binding the androgen receptor. Mol Cell Biol. 2012; 32:3190–202. [PubMed: 22665497]
22. Qi H, Fillion C, Labrie Y, Grenier J, Fournier A, Berger L, et al. AIbZIP, a novel bZIP gene located on chromosome 1q21.3 that is highly expressed in prostate tumors and of which the expression is up-regulated by androgens in LNCaP human prostate cancer cells. Cancer Res. 2002; 62:721–33. [PubMed: 11830526]
23. Hai T, Wolfgang CD, Marsee DK, Allen AE, Sivaprasad U. ATF3 and stress responses. Gene Expr. 1999; 7:321–35. [PubMed: 10440233]
24. Udayakumar TS, Hachem P, Ahmed MM, Agrawal S, Pollack A. Antisense MDM2 enhances E2F1-induced apoptosis and the combination sensitizes androgen-sensitive [corrected] and androgen-insensitive [corrected] prostate cancer cells to radiation. Mol Cancer Res. 2008; 6:1742–54. [PubMed: 19010821]
25. Saramaki OR, Harjula AE, Martikainen PM, Vessella RL, Tammela TL, Visakorpi T. TMPRSS2:ERG fusion identifies a subgroup of prostate cancers with a favorable prognosis. Clin Cancer Res. 2008; 14:3395–400. [PubMed: 18519769]
26. Ashlock BM, Ma Q, Issac B, Mesri EA. Productively infected murine Kaposi's sarcoma-like tumors define new animal models for studying and targeting KSHV oncogenesis and replication. PLoS One. 2014; 9:e87324. [PubMed: 24489895]
27. Rosenblatt AE, Burnstein KL. Inhibition of androgen receptor transcriptional activity as a novel mechanism of action of arsenic. Mol Endocrinol. 2009; 23:412–21. [PubMed: 19131511]
28. Udayakumar TS, Stoyanova R, Hachem P, Ahmed MM, Pollack A. Adenovirus E2F1 overexpression sensitizes LNCaP and PC3 prostate tumor cells to radiation in vivo. Int J Radiat Oncol Biol Phys. 2011; 79:549–58. [PubMed: 21195876]
29. Kirstein SL, Atienza JM, Xi B, Zhu J, Yu N, Wang X, et al. Live cell quality control and utility of real-time cell electronic sensing for assay development. Assay Drug Dev Technol. 2006; 4:545–53. [PubMed: 17115925]
30. Reutelingsperger CP. Annexins: key regulators of haemostasis, thrombosis, and apoptosis. Thromb Haemost. 2001; 86:413–9. [PubMed: 11487032]
31. Fan F, Jin S, Amundson SA, Tong T, Fan W, Zhao H, et al. ATF3 induction following DNA damage is regulated by distinct signaling pathways and over-expression of ATF3 protein suppresses cells growth. Oncogene. 2002; 21:7488–96. [PubMed: 12386811]
32. Nieto-Miguel T, Fonteriz RI, Vay L, Gajate C, Lopez-Hernandez S, Mollinedo F. Endoplasmic reticulum stress in the proapoptotic action of edelfosine in solid tumor cells. Cancer Res. 2007; 67:10368–78. [PubMed: 17974980]

33. Ha S, Ruoff R, Kahoud N, Franke TF, Logan SK. Androgen receptor levels are upregulated by Akt in prostate cancer. Endocr Relat Cancer. 2011; 18:245–55. [PubMed: 21317204]
34. Lin HK, Yeh S, Kang HY, Chang C. Akt suppresses androgen-induced apoptosis by phosphorylating and inhibiting androgen receptor. Proceedings of the National Academy of Sciences of the United States of America. 2001; 98:7200–5. [PubMed: 11404460]
35. Gao Y, Ishiyama H, Sun M, Brinkman KL, Wang X, Zhu J, et al. The alkylphospholipid, perifosine, radiosensitizes prostate cancer cells both in vitro and in vivo. Radiat Oncol. 2011; 6:39. [PubMed: 21496273]
36. Hu R, Isaacs WB, Luo J. A snapshot of the expression signature of androgen receptor splicing variants and their distinctive transcriptional activities. Prostate. 2011; 71:1656–67. [PubMed: 21446008]
37. Tian TV, Tomavo N, Huot L, Flourens A, Bonnelye E, Flajollet S, et al. Identification of novel TMPRSS2:ERG mechanisms in prostate cancer metastasis: involvement of MMP9 and PLXNA2. Oncogene. 2014; 33:2204–14. [PubMed: 23708657]
38. Saxena P, Trerotola M, Wang T, Li J, Sayeed A, Vanoudenhove J, et al. PSA regulates androgen receptor expression in prostate cancer cells. Prostate. 2012; 72:769–76. [PubMed: 21956655]
39. Oettgen P, Finger E, Sun Z, Akbarali Y, Thamrongsak U, Boltax J, et al. PDEF, a novel prostate epithelium-specific ets transcription factor, interacts with the androgen receptor and activates prostate-specific antigen gene expression. J Biol Chem. 2000; 275:1216–25. [PubMed: 10625666]
40. Kirby M, Hirst C, Crawford ED. Characterising the castration-resistant prostate cancer population: a systematic review. Int J Clin Pract. 2011; 65:1180–92. [PubMed: 21995694]
41. Vink SR, van Blitterswijk WJ, Schellens JH, Verheij M. Rationale and clinical application of alkylphospholipid analogues in combination with radiotherapy. Cancer Treat Rev. 2007; 33:191–202. [PubMed: 17287087]
42. Alderliesten MC, Klarenbeek JB, van der Luit AH, van Lummel M, Jones DR, Zerp S, et al. Phosphoinositide phosphatase SHIP-1 regulates apoptosis induced by edelfosine, Fas ligation and DNA damage in mouse lymphoma cells. Biochem J. 2011; 440:127–35. [PubMed: 21793801]
43. Reis-Sobreiro M, Roue G, Moros A, Gajate C, de la Iglesia-Vicente J, Colomer D, et al. Lipid raft-mediated Akt signaling as a therapeutic target in mantle cell lymphoma. Blood Cancer J. 2013; 3:e118. [PubMed: 23727661]
44. Heemers HV, Tindall DJ. Androgen receptor (AR) coregulators: a diversity of functions converging on and regulating the AR transcriptional complex. Endocr Rev. 2007; 28:778–808. [PubMed: 17940184]
45. Lu D, Wolfgang CD, Hai T. Activating transcription factor 3, a stress-inducible gene, suppresses Ras-stimulated tumorigenesis. J Biol Chem. 2006; 281:10473–81. [PubMed: 16469745]
46. Wang Z, Xu D, Ding HF, Kim J, Zhang J, Hai T, et al. Loss of ATF3 promotes Akt activation and prostate cancer development in a Pten knockout mouse model. Oncogene. 2014
47. Hai T, Hartman MG. The molecular biology and nomenclature of the activating transcription factor/cAMP responsive element binding family of transcription factors: activating transcription factor proteins and homeostasis. Gene. 2001; 273:1–11. [PubMed: 11483355]
48. Antonarakis ES, Lu C, Wang H, Luber B, Nakazawa M, Roeser JC, et al. AR-V7 and resistance to enzalutamide and abiraterone in prostate cancer. N Engl J Med. 2014; 371:1028–38. [PubMed: 25184630]
49. Maughan BL, Antonarakis ES. Androgen pathway resistance in prostate cancer and therapeutic implications. Expert Opin Pharmacother. 2015; 16:1521–37. [PubMed: 26067250]

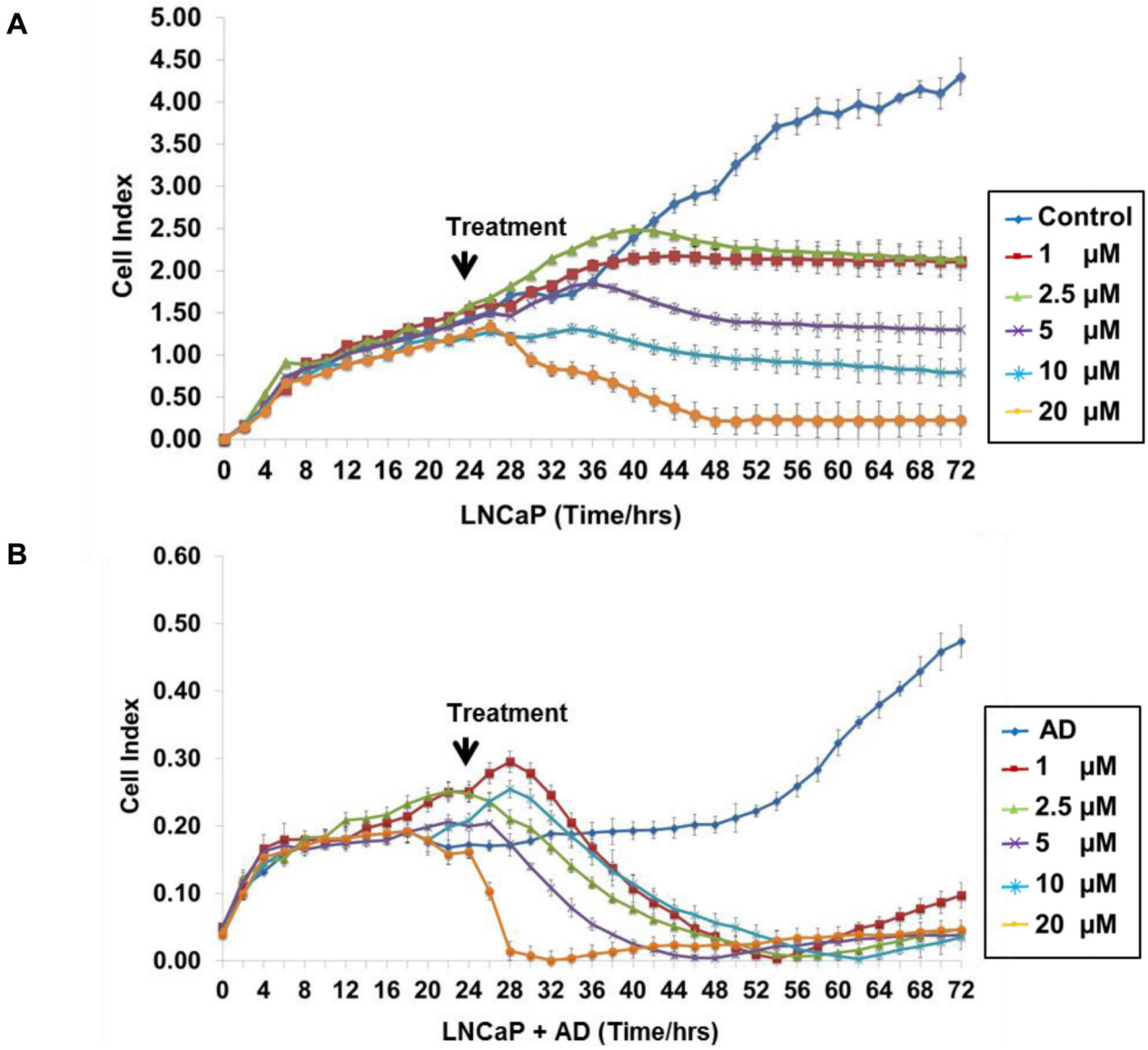

Figure 1. Edelfosine and AD inhibits cell proliferation in LNCaP cells

LNCaP cells (2×10^4) were grown in E-Plates for 24 h in complete or AD medium. Cells were treated with edelfosine (1, 2.5, 5, 10 and 20 μM) with appropriate control groups (A) LNCaP and (B) LNCaP + AD. Cells were monitored and cell proliferation was measured in real time by RTCA cell proliferation assay and the average cell index is shown for 72 h. Each data point is represented by mean ± SD (n =3).

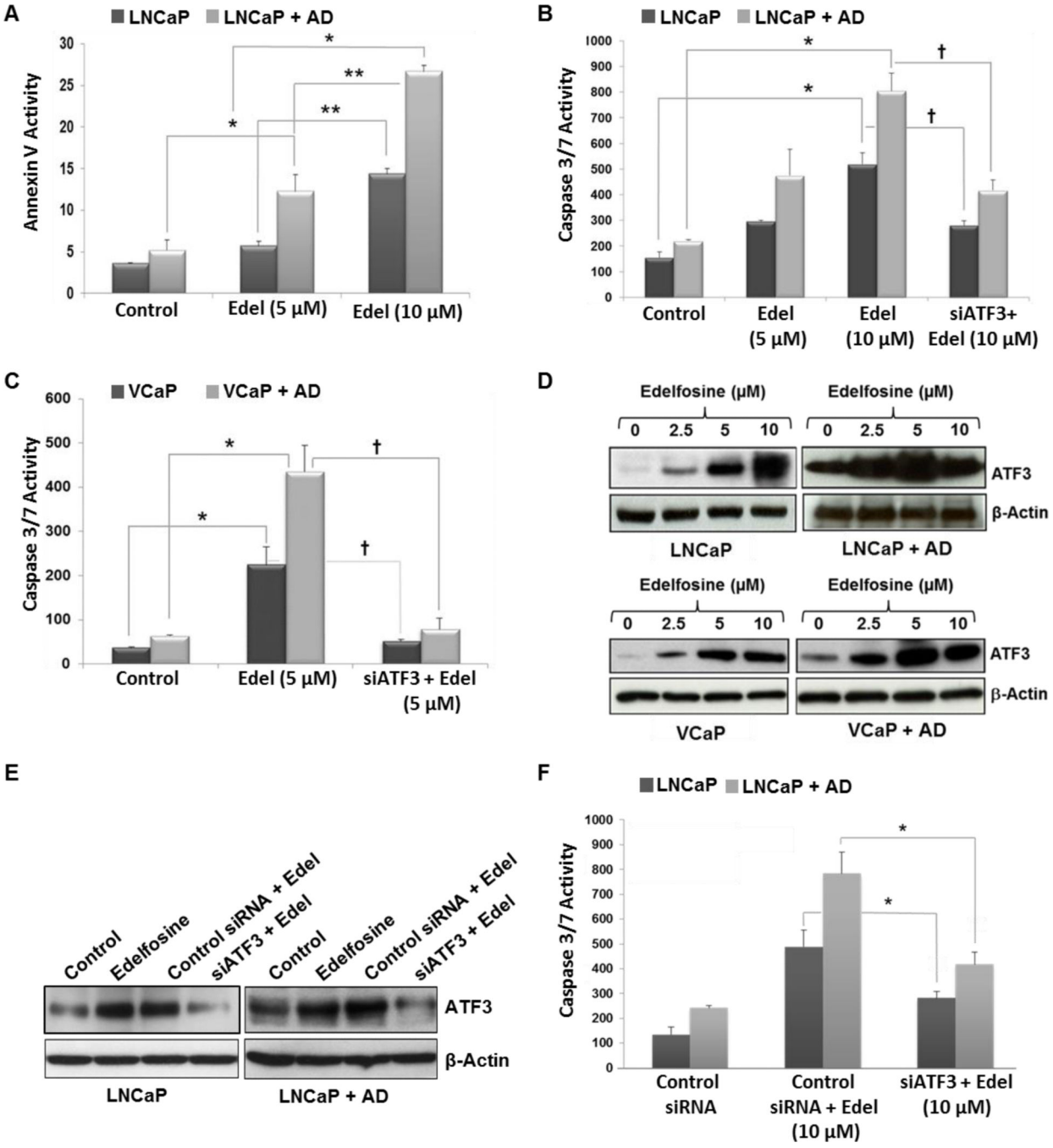

Figure 2. ATF3 knockdown via siATF3 inhibits apoptosis in prostate cancer cells after AD and edelfosine treatment

LNCaP cells were grown for 3 days in complete or AD medium and treated with edelfosine (5 μM and 10 μM) alone or in combination with AD for Annexin V staining. (A) Treated cells were harvested after 24 h and stained using the Guava Nexin kit. Percentage of Annexin V positive cells was measured by flow cytometric analysis and the data processed using CytoSoft software. (B) LNCaP and (C) VCaP cells were harvested 24 hours following treatment and caspase 3/7 activity was determined using the Apo-ONE™ Homogeneous caspase 3/7 assay kit. For ATF3 knockdown, both LNCaP and VCaP cells grown in

complete or AD medium were transfected with siATF3 (10 nM), followed by treatment with edelfosine (5 or 10 μM). (D) LNCaP and VCaP cells were grown as described above and were treated with AD and/or edelfosine (0, 2.5, 5 and 10 μM). Treated cells were harvested after 24 h; total proteins were examined by Western immunoblotting for ATF3 expression levels. The same blot was stripped and re-probed for β-actin. (E) ATF3 knockdown via siATF3 (10 nM), after edelfosine (10 μM) treatment was confirmed by Western blot analysis using AFT3 specific antibodies. (F) LNCaP cells were transfected with control siRNA or siATF3 (10 nM), followed by edelfosine (10 μM) treatment, caspase 3/7 activity was measured. Data shown represent the mean ± SD from three independent experiments. *$p < 0.05$, compared to respective control, **$p < 0.05$, compared to edelfosine 5 μM (one way ANOVA, Bonferroni test).

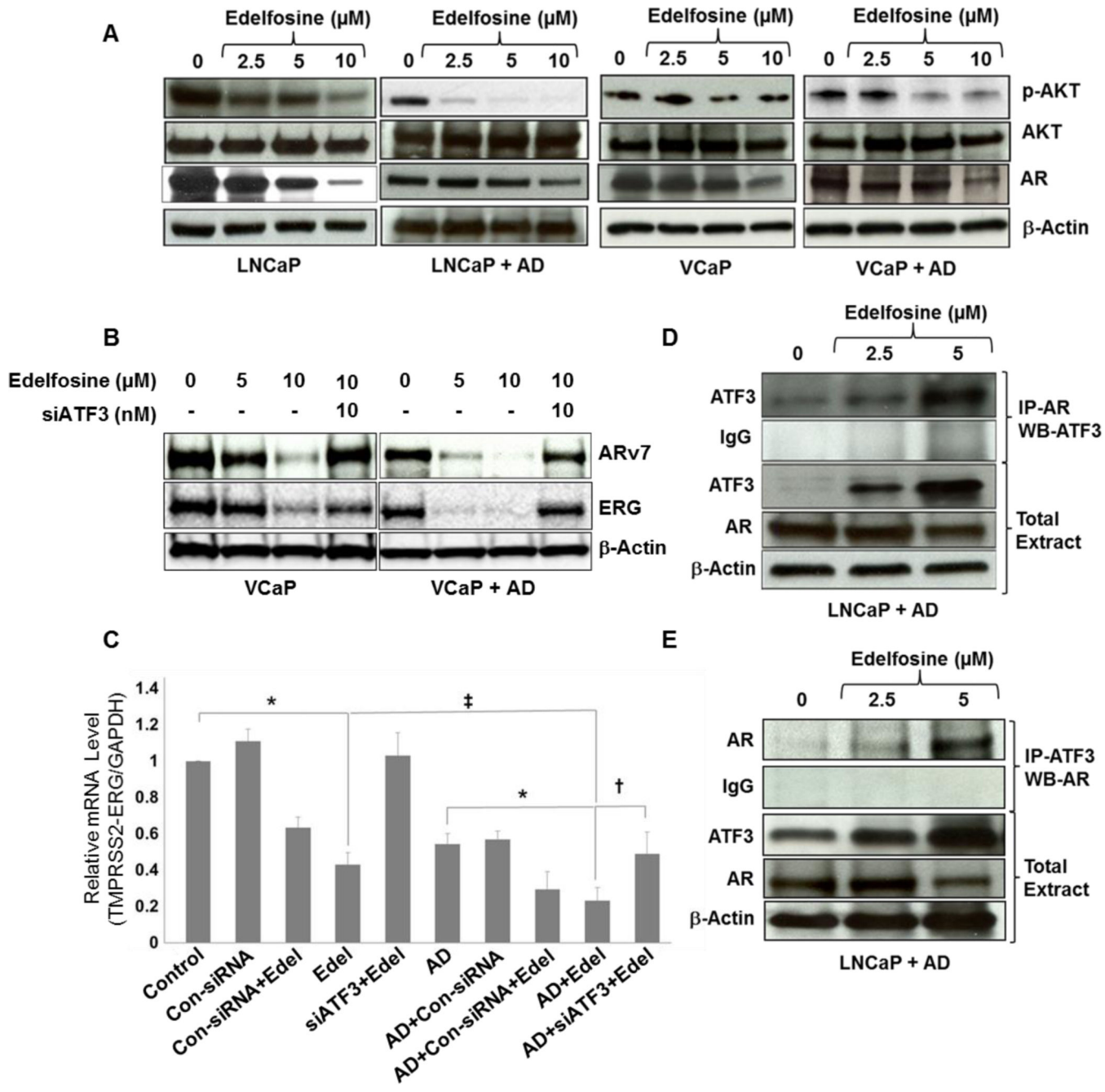

Figure 3. Changes in AKT, AR, ARv7 and ERG protein levels after AD and edelfosine treatments

(A) LNCaP and VCaP cells were cultured in complete or AD medium for 3 days in 10 cm tissue culture dishes and then treated with edelfosine (0, 2.5, 5 and 10 μM). Treated cells were harvested after 24 h, whole-cell lysates were extracted, and the expression of p-AKT, total AKT and AR were determined by Western blotting. The same blot was probed again for β-actin. (B) VCaP cells grown in complete or AD medium were pre-transfected with siATF3 (10 nM) for 18 h in the presence of lipofectin reagent followed by edelfosine (0, 5 and 10 μM) treatment. Whole-cell lysates were extracted from treated cells after 24 h. ARv7

and ERG expression was determined by Western blotting and the same blot was stripped and re-probed for β-actin. (C) Relative mRNA levels of TMPRSS2-ERG gene product ERG in VCaP cells. Real-time PCR was performed using total RNA extracted from VCaP cells. The cells grown in CM or AD media were treated with edelfosine (10 μM), siATF3 or control siRNA (10 nM) either alone or in combination with edelfosine. The results were normalized to the expression of GAPDH and presented as relative mRNA expression levels (mean ± SD, n = 3). *$p < 0.001$, compared to respective controls, $^{‡}p < 0.05$, compared to edelfosine alone, $^{†}p < 0.05$, compared to AD + edelfosine (one-way ANOVA). (D) ATF3 interaction with AR. AD and edelfosine (0, 2.5 and 5 μM) treated whole-cell lysates were co-immunoprecipitated with antibodies against AR, followed by Western blot analysis with antibodies specific for ATF3. (E) Reverse immunoprecipitation was carried out in the AD and edelfosine (0, 2.5 and 5 μM) treated whole-cell lysates to confirm the interaction between ATF3 and AR.

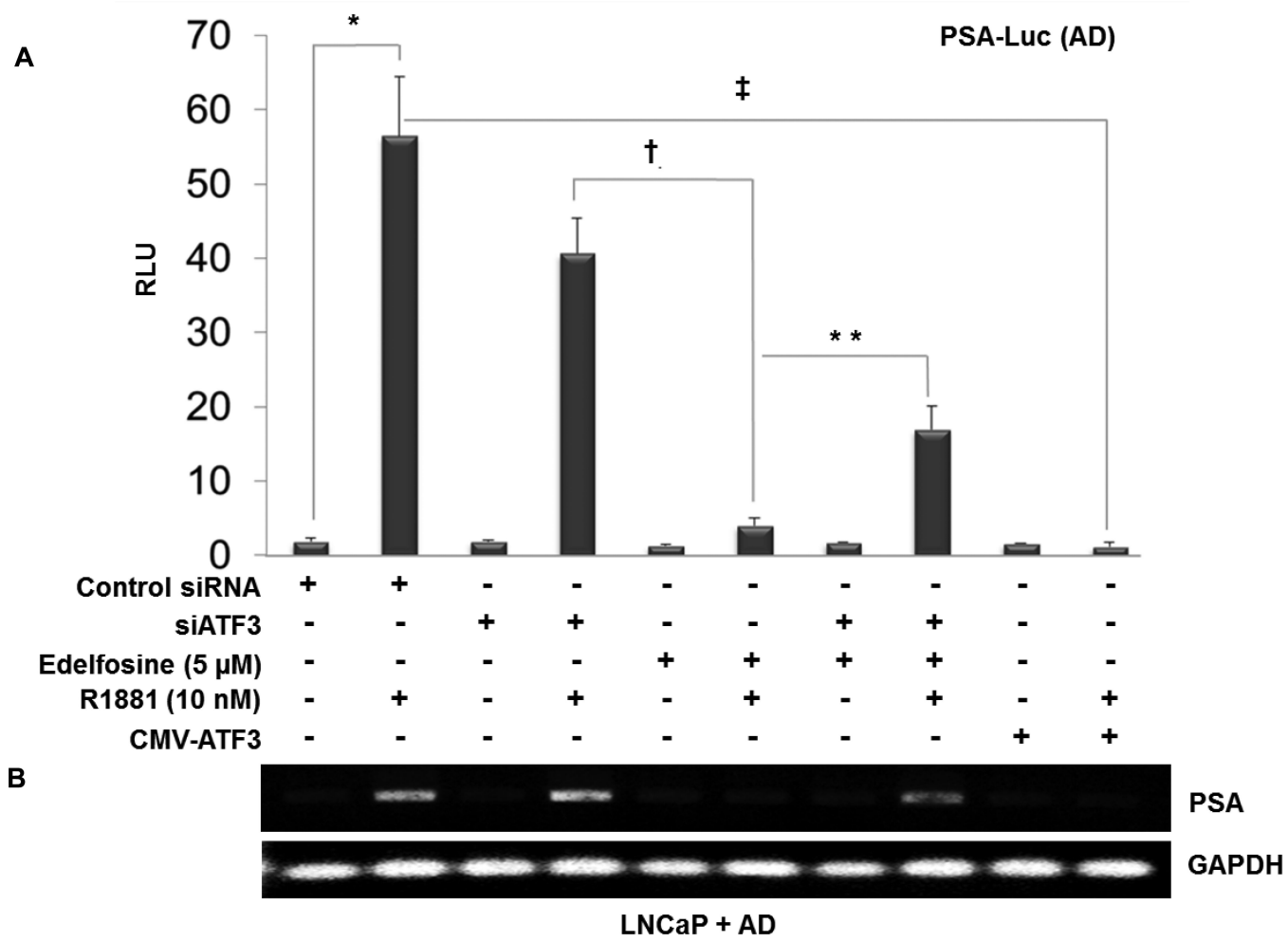

Figure 4. ATF3 represses AR transcriptional target PSA in LNCaP cells after AD and edelfosine treatment

Androgen deprived LNCaP cells were co-transfected with PSA-luciferase reporter constructs (3 μg/well), CMV-ATF3 (3 μg), siATF3 or control siRNA (10 nM). To normalize the transfection efficiency, cells were co-transfected with renilla luciferase (30 ng/well). Following 3 h transfection the cells were treated with edelfosine (5 μM) and R1881 (10 nM). Cells were harvested 24 h post treatment, lysed and assayed for luciferase activity using the dual- luciferase reporter gene assay system. The data represents the ratio between firefly/ renilla luciferase activities (mean ± SD, n = 3). *$p < 0.001$, compared to group without R1881, $^{‡}p < 0.05$, compared to R1881 alone, $^{†}p < 0.05$, compared to group with siATF3, **$p < 0.05$, compared to group without siATF3 (one way ANOVA). (B) RT-PCR analysis for PSA mRNA expression. Parallel experiments were done with the treatment groups as in Figure 4A. Total RNA (2 μg) was reverse transcribed and the cDNA product was PCR amplified using PSA and GAPDH primers. A portion (10 μl from a 20 μl volume) of the PCR reaction product was electrophoresed on a 1.5% agarose gel. Electrophoresed and ethidium bromide stained PCR products from RT–PCR reactions were recorded under UV-transillumination using the Gel Doc XR system (Bio-Rad, Hercules, CA). RNA content was normalized with respect to the amount of GAPDH product.

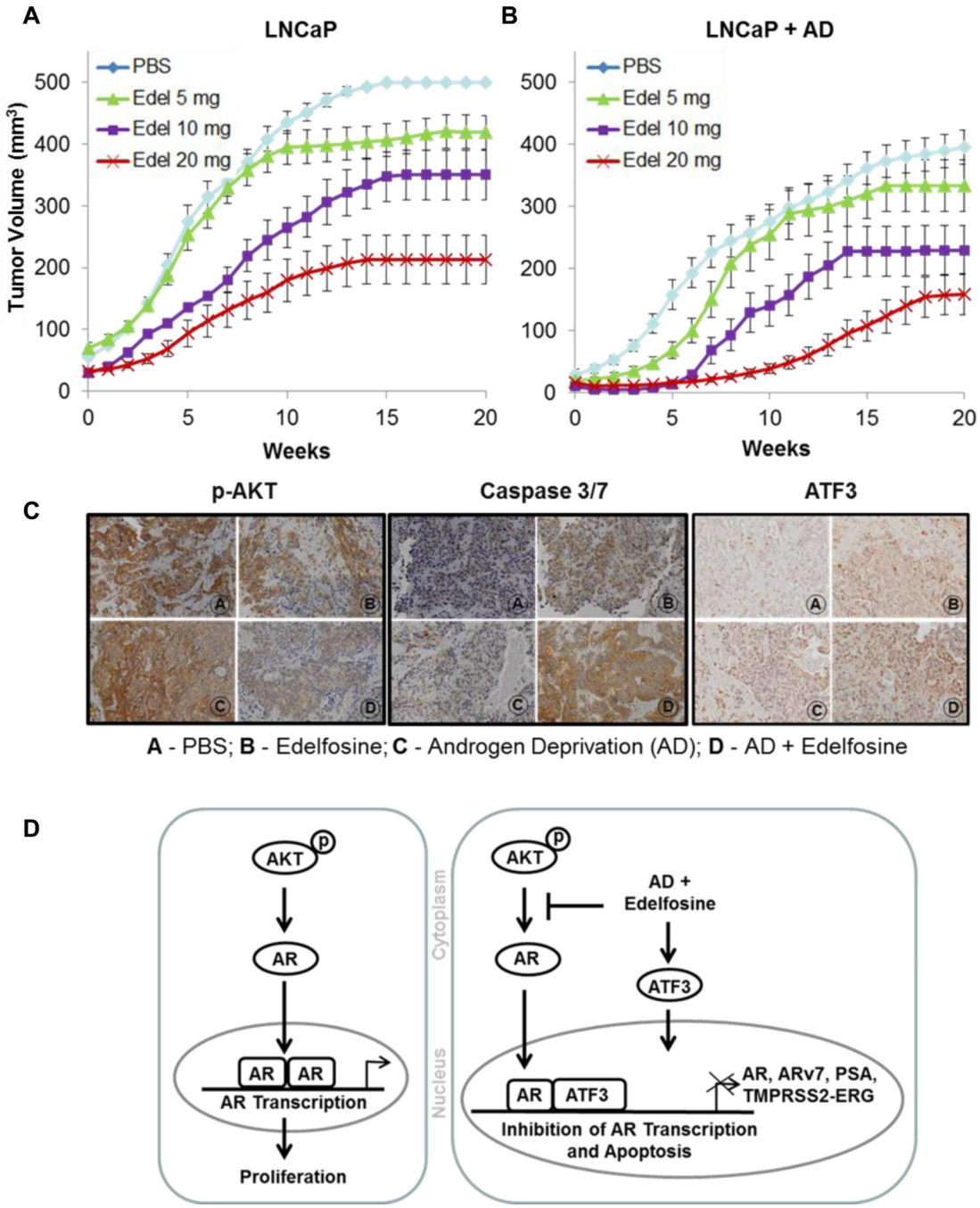

Figure 5. Growth curves showing *in vivo* tumor growth inhibition after AD and edelfosine treatment

LNCaP cells (5×10^5) were implanted into the dorsal prostate of athymic nude mice (n = 9 - 13). Two weeks after tumor implantation, serum PSA levels were measured weekly. Mice in the group without AD were treated orally by gavage when the PSA levels are between 3.0 – 8.0 ng/ml. For the groups with AD bilateral orchiectomy was performed 3 days prior to edelfosine treatment. A total of eight groups of animals were studied: PBS (control) and three concentrations of edelfosine were given at doses 5, 10 and 20 mg/kg, 3 days per week for 10 weeks, with and without AD. Post-treatment tumor volume and weekly serum PSA

levels were determined by MRI and ELISA respectively. The curves and bars represent mean ± SEM of numerical fits of tumor growth curves for individual animals. (A) Edelfosine alone; and (B) Edelfosine combined with AD. (C) Expression of p-AKT, caspase 3/7 and ATF3 after AD and edelfosine (20 mg/kg) treatments *in vivo*. Orthotopically grown LNCaP tumors was excised 24 h after the treatment and were processed for immunohistochemistry. The sections were stained for p-AKT, caspase 3/7 and ATF3. (Panel A -PBS; Panel B - Edelfosine; Panel C - Androgen deprivation (AD); Panel D - AD + Edelfosine). Images were scanned and captured with a VS120-SL microscope. Magnification x20. (D) Schematic representation of AD and edelfosine mediated increase in ATF3 that interacts with AR, leading to the repression of AR-transcriptional activity and its downstream targets such as PSA, ARv7 and TMPRSS2-ERG fusion gene in prostate cancer cells.

Table 1

PSA and Tumor Volume (mean ± SEM) of orthotopically grown LNCaP tumors at 6 weeks following AD + Edelfosine treatments (n = 9 -13).

Group	TV (mm^3)	PSA (ng/ml)	% of mice with TV<100 mm^3 (no./total)	% of mice with PSA <25 ng/ml (no./total)	% combined (no./total)	*TV doubling time (weeks)	*PSA doubling time (weeks)
PBS	314 ± 52	91 ± 7	10% (1/10)	10% (1/10)	10% (1/10)	2.77 ± 0.4	2.40 ± 0.2
Edel (20 mg)	192 ± 63†	39 ± 12†	60% (6/10)†	50% (5/10)†	50% (5/10)†	6.49 ± 1.3†	5.83 ± 1.2†
PBS + AD	112 ± 52	30 ± 12	80% (8/10)	60% (6/10)	60% (6/10)	3.94 ± 1.1	3.51 ± 1.1
Edel (20 mg) + AD	15 ± 6†,‡	2 ± 1†,‡	100% (11/11)	100% (11/11)†,‡	100% (11/11)†,‡	7.63±1.0†	7.94 ± 1.1†

Tumor parameters were calculated by kinetic modeling of longitudinal data from PSA and tumor volume. PSA and TV values for fast growing tumors are truncated at 100 ng/ml and/or 500 mm^3, respectively.

Abbreviations:

AD, androgen deprivation; PSA, prostate specific antigen; TV, tumor volume; PBS, phosphate buffered saline; Edel – edelfosine.

*Tumor doubling times were calculated from fitted data for mice where TV and PSA exhibit an upward trend after treatment. For the rest of the animals 10 weeks is assumed.

†Statistically significant difference ($p < 0.05$), compared to the PBS group.

‡Statistically significant difference ($p < 0.05$), compared to all groups.